ARTICLE

A Thermoplastic/Thermoset Blend Exhibiting Thermal Mending and Reversible Adhesion

Xiaofan Luo,[†] Runqing Ou,[‡] Daniel E. Eberly,[‡] Amit Singhal,[‡] Wantinee Viratyaporn,[§] and Patrick T. Mather*,[†]

Syracuse Biomaterials Institute and Department of Biomedical and Chemical Engineering, Syracuse University, Syracuse, New York 13244, NEI Corporation, 400 Apgar Drive, Suite E, Somerset, New Jersey 08873, and Department of Materials Science & Engineering, Rutgers University, Piscataway, New Jersey 08873

ABSTRACT In this paper, we report on the development of a new and broadly applicable strategy to produce thermally mendable polymeric materials, demonstrated with an epoxy/poly(ϵ-caprolactone) (PCL) phase-separated blend. The initially miscible blend composed of 15.5 wt % PCL undergoes polymerization-induced phase separation during cross-linking of the epoxy, yielding a "bricks and mortar" morphology wherein the epoxy phase exists as interconnected spheres (bricks) interpenetrated with a percolating PCL matrix (mortar). The fully cured material is stiff, strong, and durable. A heating-induced "bleeding" behavior was witnessed in the form of spontaneous wetting of all free surfaces by the molten PCL phase, and this bleeding is capable of repairing damage by crack-wicking and subsequent recrystallization with only minor concomitant softening during that process. The observed bleeding is attributed to volumetric thermal expansion of PCL above its melting point in excess of epoxy brick expansion, which we term differential expansive bleeding (DEB). In controlled thermal-mending experiments, heating of a cracked specimen led to PCL extrusion from the bulk to yield a liquid layer bridging the crack gap. Upon cooling, a "scar" composed of PCL crystals formed at the site of the crack, restoring a significant portion of the mechanical strength. When a moderate force was applied to assist crack closure, thermal-mending efficiencies exceeded 100%. We further observed that the DEB phenomenon enables strong and facile adhesion of the same material to itself and to a variety of materials, without any requirement for macroscopic softening or flow.

KEYWORDS: polymerization-induced phase separation • epoxy • self-healing • fracture • adhesion

INTRODUCTION

Polymeric materials, such as high-performance thermosets, adhesives, coatings, and elastomers, are susceptible to damage in the form of cracking or microcracking, resulting in a significant shortening of the service lifetime. Inspired by biological systems where specific mechanisms can be triggered to automatically repair damage, thereby restoring the strength and function, substantial efforts have been undertaken to incorporate this ability to "self-heal" within polymeric materials as a built-in material functionality. One of the approaches is to initiate a specific chemical reaction, usually polymerization, locally at the damage site. This requires the incorporation of microscopic "containers" that host the reactive species and prevent them from predamage reaction. Some successful examples of such container designs include microspheres and hollow fibers, encapsulated or infiltrated with different reactive species including dicyclopentadiene monomer (1−4), functionalized poly(dimethylsiloxane) (5, 6), and epoxy resins (7−11). For all such cases, the reactive monomer is released upon rupture of the container during the propagation of a crack. Subsequent flow leads to contact with a catalyst or hardener, either dispersed in the resin matrix or from other ruptured containers, and initiation of the polymerization. This approach, despite the sophistication in chemistry and manufacturing, has been quite successful in achieving high mending efficiencies and is applicable to various types of polymeric materials including fiber-reinforced composites (1, 7, 8), composite sandwich structures (9), and elastomers (5). Recently, researchers have reported on the possibility of building a three-dimensional network of channels (instead of separated containers) to store the healing agent, mimicking the vascular structure in biological bodies (12), and affording repeated mending cycles. Aside from polymerization-based mending, reversible chemistry, such as covalently bonded networks by Diels−Alder reaction (13) and hydrogen-bonded supramolecular networks (14), has been ingeniously utilized for producing mendable polymeric materials. Through control of the reaction conditions, the fractured networks can be reconstructed and thus mended at the molecular level. However, this strategy is limited to only a narrow set of less commonly used polymers, rendering broad utilization of the technology unlikely. Some other mending approaches for polymers include solvent encapsulation (15), *miscible* thermoset/thermoplastic blending (16), and nanoparticle aggregation (17). Interested readers are directed to a number of review articles that appeared recently (18−22).

While representing significant advances, the existing mendable polymer technologies present profound chal-

* To whom correspondence should be addressed. E-mail: ptmather@syr.edu. Tel: (315) 443-8760. Fax: (315) 443-9175.
Received for review November 2, 2008 and accepted January 15, 2009
[†] Syracuse University.
[‡] NEI Corp.
[§] Rutgers University.
DOI: 10.1021/am8001605

Published on Web 02/11/2009

Scheme 1. Chemical Structures of DGEBA, DDS, and PCL

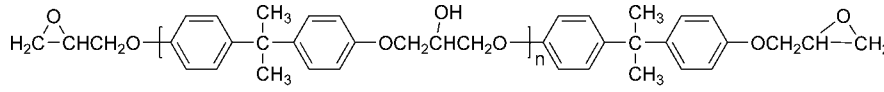

Diglycidyl ether of bisphenol-A (DGEBA; epoxide equivalent weight = 172~176)

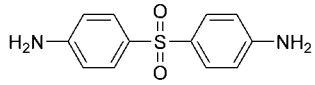

4,4'-diaminodiphenylsulfone (DDS)

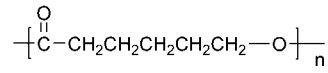

Poly(caprolactone) (PCL)

lenges for commercialization owing to raw material cost and process complexity. Alternative approaches that are intrinsically low in cost and capable of large-scale industrial production are needed; this has motivated our research efforts. For our approach, we further sought a "biphasic" structure: (i) a major "load-bearing" phase that has good stiffness and strength to perform major mechanical and structural functions and (ii) a "healing" phase of a thermoplastic healing agent to repair the material to restore its mechanical and structural integrity after being damaged. Ideally, the healing phase should have a large degree of interpenetration with the major phase to maximize its coverage with little compromise in the overall material properties. Satisfying the constraint of low cost and scalability, we have restricted ourselves to commercially available polymers, including epoxy resin and poly(ϵ-caprolactone) (PCL), and a simple manufacturing process.

In this report, we will show that polymerization-induced phase separation (PIPS) was utilized to fabricate the desired biphasic structure. PIPS is a well-studied process to produce phase-separated polymer blends, used in the past to toughen brittle thermosets. Other applications have included polymer-dispersed liquid crystals (23), macroporous thermosets (24), and microencapsulation (25). The interested reader is directed to several comprehensive reviews that have appeared (26−28). Epoxy/PCL blends are known to undergo PIPS when cured with 4,4′-diaminodiphenylsulfone (DDS), owing to a competition between inter- and intramolecular hydrogen bonding with this molecule (29−31). In what follows, we present the processing protocol and resultant properties of unique mending and bonding for specific epoxy/PCL blends. We further present an explanation for the properties in light of the combination of a unique morphology and heating-induced flow and diffusion of the PCL component.

EXPERIMENTAL SECTION

Materials. Diglycidyl ether of Bisphenol A (DGEBA; epoxide equivalent weight = 172−176), 4,4′-diaminodiphenylsulfone (DDS), and poly(ϵ-caprolactone) (PCL; $M_n \sim$ 42 500 g/mol and $M_w \sim$ 65 000 g/mol) were purchased from Aldrich and used as received. The chemical structures are shown in Scheme 1.

Blend Preparation Technique. The DGEBA liquid resin and PCL pellets in different mass ratios of m_{DGEBA}:m_{PCL} = 90:10, 85:15, 80:20, 70:30, and 60:40 were first melt-mixed at 120 °C by continuous mechanical stirring at 100−200 rpm using an Arrow 850 stirrer with a Teflon stirring blade for 1−2 h. The temperature was increased to 140 °C and the curing agent DDS (crystalline) powder then added, using a molar ratio of DGEBA:DDS = 2:1. The mechanical stirring lasted for another several minutes until the mixture became clear and transparent, indicating a single phase. The mixture was then degassed at 120 °C to remove all trapped air bubbles, poured into a silicone rubber mold, and cured at 180 °C for 3 h. Table 1 provides the nomenclature adopted for samples studied, along with their associated epoxy/PCL mass ratio.

Table 1. Summary of Blend Compositions Studied

sample name[a]	m_{DGEBA}:m_{PCL}
epoxy/PCL(4.3)	90:10
epoxy/PCL(11.5)	85:15
epoxy/PCL(15.5)	80:20
epoxy/PCL(27.0)	70:30
epoxy/PCL(34.9)	60:40

[a] The numbers in parentheses indicate the percentage weight fractions of PCL in the blend (DGEBA + DDS + PCL).

Thermal Analysis. Differential scanning calorimetry (DSC) experiments were conducted using a TA Q100 instrument equipped with a refrigerated cooling accessory under a nitrogen purge. Fragments from cured bars were first heated to 200 °C, then cooled to −80 °C, and finally heated to 240 °C to collect heat flow data. Heating and cooling rates were 10 °C/min.

Dynamic Mechanical Analysis. A TA Q800 dynamic mechanical analyzer was used to measure the temperature-dependent linear viscoelastic properties of selected samples. For each case, a rectangular sample bar with dimensions of 17.4 mm × 10 mm × 2.8 mm was used under single-cantilever mode. The sample was subjected to an oscillatory deflection with a displacement amplitude of 15 μm at a frequency of 1 Hz, while the temperature was ramped from −90 to +280 °C at a constant heating rate of 3 °C/min for measurements of the storage modulus, loss modulus, and loss tangent. The transition temperatures (T_m and T_g) were determined as the onset point of the tensile storage modulus (E') decreases.

Morphological Characterization. The morphologies of fully cured samples were characterized using scanning electron microscopy (SEM) and polarized optical microscopy (POM). For SEM, a fully cured sample bar was first immersed in liquid nitrogen and quickly fractured. The fractured surface was then treated with chloroform to selectively etch away the PCL component, sputter-coated with gold and examined by a Philips XL30 SEM instrument. For POM, a thin film of uncured mixture was sandwiched between a glass slide and a coverslip and fully cured at 180 °C for 3 h. An Olympus BX51 optical microscope with perpendicularly oriented polarizer and analyzer was used to visualize the phase morphology.

Visualization of "Bleeding". A Zeiss Discovery V8 stereomicroscope was used to visualize the "bleeding" process using a magnification of 8× and oblique reflective illumination. Sample bars were coated with a thin layer of gold (1−3 nm thick) to enhance the contrast and placed on a customized heated stage.

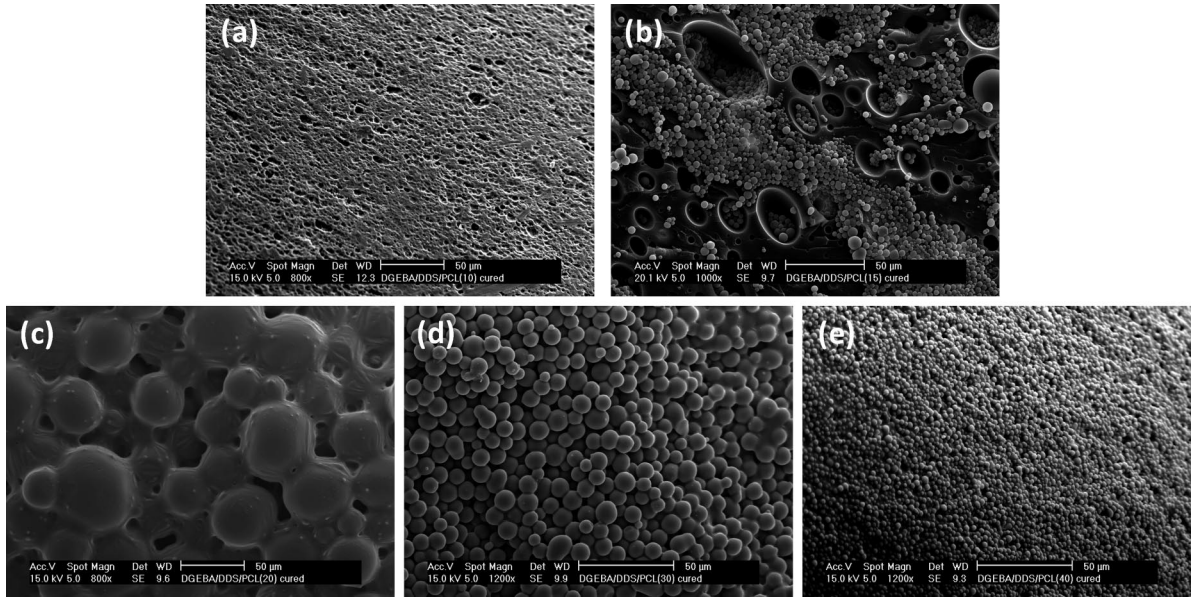

FIGURE 1. SEM images showing the bulk morphologies of fully cured epoxy/PCL blends of different compositions: (a) epoxy/PCL(4.3), (b) epoxy/PCL(11.5), (c) epoxy/PCL(15.5), (d) epoxy/PCL(27.0); (e) epoxy/PCL(34.9).

The surface temperature of the sample bar was recorded using a DATAQ DI-5B47 linearized thermocouple input module with a T-type thermocouple through a DI-195 data acquisition board. WinDaq/Lite software was used to analyze the acquired temperature profile. Digital video microscopy movies were taken at a constant frame rate of 1 frame/s.

Characterization of Thermal-Mending Efficiency. Thermal-mending efficiencies were characterized by fracture experiments guided by ASTM D5045 using the single-edge-notched-beam (SENB) geometry, noting that strict adherence to this standard was not possible because of the ductile failure behavior of our samples. For virgin and thermally mended specimens (described below), each notched sample bar (4 mm × 10 mm × 35 mm; notch = 1.5 mm) was loaded to failure (defined as the point at which a 90% drop of the maximum load is achieved) under a three-point bending mode at a constant crosshead speed of 10 mm/min. Generally, specimens did not completely break into halves in a brittle fashion, and tests were terminated at a point that yielded a short ligament of approximately 10% of the sample width in dimension. Such fractured specimens were next placed in a vertically oriented Teflon die with or without an axial load applied, with the former achieved by mounting a calibrated weight on the top. Thermal mending was conducted by placing the Teflon die in a convective oven isothermal at 190 °C and holding it there for 8 min. Specimens were then allowed to cool to room temperature and tested again to failure in three-point bending at the same crosshead speed. No changes in the notch geometry were observed before and after thermal mending. Pre- and post-mending load−displacement curves were compared to calculate a thermal-mending efficiency, here defined in two ways (both are reported): (i) ratio of postmending to premending strain energy to failure, determined as the area under each load−displacement curve, or (ii) ratio of postmending to premending peak loads measured during specimen fracture. Fracture toughness values, per se, are not reported because of the ductile failure observed.

Fractography Studies. A JEOL JSM-5600 scanning electron microscope was used to study the fracture mode and crack repairing mechanism. A typical voltage of 10 kV was applied in all of the experiments. SENB specimens after first fracture, thermal mending, and second fracture were sputter-coated with gold and viewed in the instrument. Images were taken either on the top surface, where the crack was propagating, or on the fracture surface.

Characterization of Adhesive Bonding Strength. Butt-joint tests were performed to quantify the adhesive bonding strength. Two sample bars of the same dimensions (25.4 mm × 10 mm × 5 mm) were first compressively loaded on a spring-based bonding device that exerted a constant 2 N load normal to the 5 mm × 10 mm surfaces (a photograph is available in the Supporting Information). After heating in a convective oven at 150 °C for 9 min, the sample-loaded device was allowed to cool at room temperature for another 10 min before taking out the samples. The butt-joint test was performed on a MTS QTest tensile instrument, with a controlled displacement rate of 0.5 mm/min. The specimen (two sample bars bonded together) was loaded to fracture with the load−displacement data simultaneously recorded. The fractured samples were then bonded and tested under the same conditions. Three bonding−testing cycles were performed on two individual specimens (four sample bars).

RESULTS AND DISCUSSION

All epoxy/PCL blends were fully cured after 3 h at 180 °C, as indicated by the fact that no exothermic peak can be observed in the DSC heating runs in the temperature range of −50 to +240 °C (Supporting Information). A series of morphologies can be produced by varying the weight ratio of DGEBA to PCL, as shown by the SEM images in Figure 1. Note that all of the surfaces were treated with chloroform to selectively remove the PCL component; therefore, the only "visible" component on the SEM images is the epoxy. With a relatively low PCL content (**epoxy/PCL(4.3)**), epoxy forms the matrix phase with randomly dispersed PCL particles (Figure 1a). As the PCL content is slightly increased (**epoxy/PCL(11.5)**), the morphology becomes quite complex because of secondary and tertiary phase separation events occurring within the primary phase domains (29, 31). However, the primary morphology (morphology of the primary phases) is cocontinuous in nature, as is evident from the POM image shown in Figure 2a. The dark and light

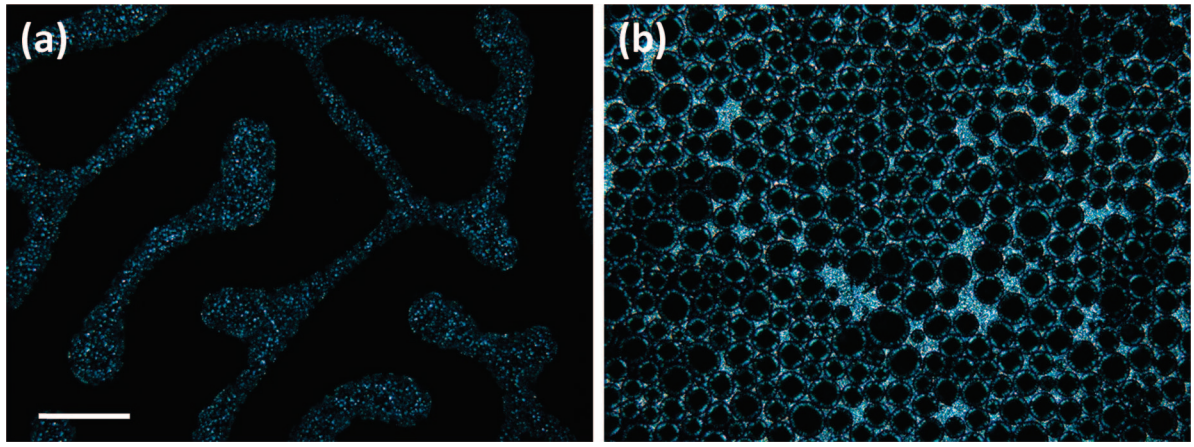

FIGURE 2. POM images for (a) epoxy/PCL(11.5) and (b) epoxy/PCL(15.5). The scale bar represents 200 μm.

(resulting from birefringence) regions are composed primarily of amorphous epoxy and semicrystalline PCL, respectively. Phase inversion happens by a further increase of PCL, where epoxy becomes the discrete phase dispersed in a continuous PCL matrix (Figures 1a–c and 2b). Also, the size of the epoxy spheres becomes smaller with further increased PCL content.

Among all compositions, **epoxy/PCL(15.5)** shows the most promising morphology for the anticipated thermal-mending application. First, PCL (the repair agent) forms a percolating, continuous phase highly interpenetrated with the epoxy phase, which ensures its presence and delivery at the local damage site regardless of where the damage takes place. Second, the epoxy, still the major component of the material (ca. 84.5 wt % of the material, considering the amount of curing agent DDS reacted with DGEBA), should dominate the mechanical properties. An important structural difference between **epoxy/PCL(15.5)** and the other two samples with higher PCL content (**epoxy/PCL(27.0)** and **epoxy/PCL(34.9)**) is that the epoxy spheres are highly interconnected (Figure 1c) and therefore can effectively bear the load as a whole entity. We term this special morphology "bricks and mortar" where "bricks" and "mortar" refer to the interconnected epoxy spheres and the continuous PCL matrix, respectively. In fact, this is the composition in which we found the best balance between the thermal-mending performance and mechanical properties and will be the major focus in the following sections.

The temperature-dependent linear viscoelastic properties of different blends as well as pure epoxy and PCL were studied by dynamic mechanical analysis (DMA). For clarity reasons, we only show the results for **epoxy/PCL(15.5)**, pure epoxy, and PCL here in Figure 3. (Others are available in the Supporting Information.) **Epoxy/PCL(15.5)** shows two distinct transitions (E' trace), corresponding to the melting of PCL (59 °C) and the glass transition of epoxy (203 °C). The close proximity of the two transition temperatures to the T_m of PCL and T_g of epoxy indicates the fact that the phase separation was complete, yielding almost pure PCL and epoxy phases. The storage modulus (E') of fully cured **epoxy/PCL(15.5)** at room temperature (25 °C) is 1.7 GPa, close to that of the epoxy (2.2 GPa) and much higher than that of

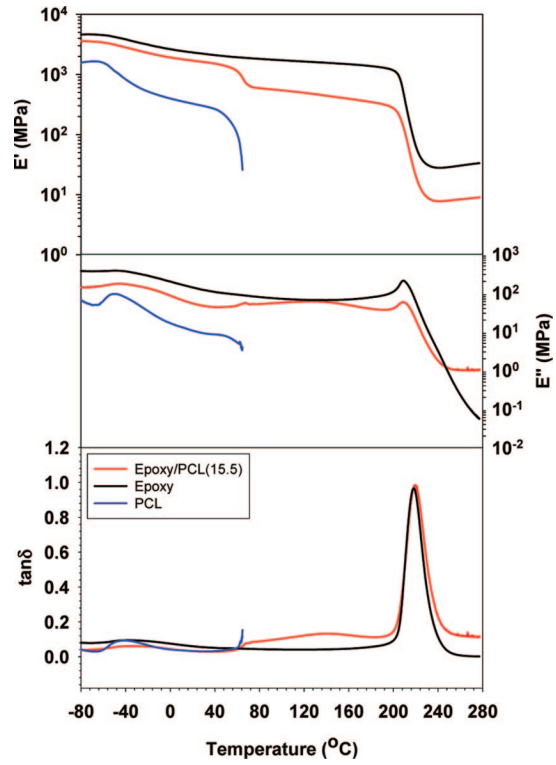

FIGURE 3. DMA results (3 °C/min; 1 Hz) of fully cured epoxy/PCL(15.5), compared with pure epoxy and PCL.

pure PCL (0.3 GPa). Even above the melting temperature of PCL, the blend still behaves as a stiff elastic solid, given the relatively low loss modulus (E'') and loss tangent (tan δ) values. Melting the PCL fraction does not fluidize the blend or induce any macroscopic flow or obvious dimensional changes, consistent with the microscopic observations of interconnectivity (Figure 1c). This behavior is dramatically different from that of pure PCL as well as epoxy/PCL blends with high PCL content (such as **epoxy/PCL(34.9)**), which lose most of the mechanical strength or even start to flow (in the case of pure PCL) when heated above T_m (Supporting Information). The observed properties of **epoxy/PCL(15.5)** also stand in contrast to *miscible* epoxy/thermoplastic blends (32) for which the glass transition temperature is lowered in proportion to the thermoplastic added and marking the onset of dramatic softening. In fact, the material remains

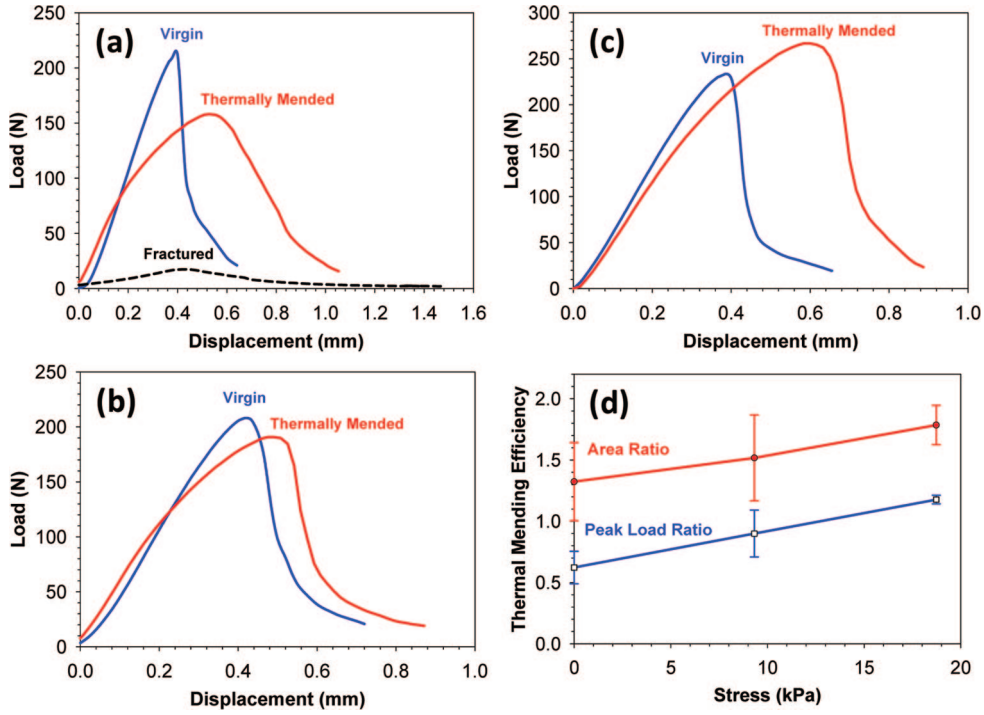

FIGURE 4. Characterization of thermal-mending efficiencies using the SENB geometry in three-point bending. Specimens were first loaded to failure and then thermally mended at 190 °C for 8 min under different compressive stresses of (a) 0, (b) 9.3, and (c) 18.7 kPa. The mended samples were tested again after cooling to room temperature. Three fractured, but unhealed, specimens were also tested, with the average load−displacement curve shown in part a as the black dashed curve. The thermal-mending efficiencies, defined as either the strain-energy-to-failure or peak load recovered relative to the virgin sample, are plotted in part d as a function of the compressive mending stress. Each point in part d represents the average of three independent test results.

stiff until 203 °C is reached, the T_g of the epoxy. The composition and morphology of **epoxy/PCL(15.5)** combine to display quite surprising mechanical properties that are dominated by the interconnected epoxy "bricks", making the material suitable for various structural functions.

Besides demonstrating desired mechanical properties, **epoxy/PCL(15.5)** also showed surprisingly good thermal-mending capability. Fracture experiments following ASTM D5045 using the SENB geometry were conducted to quantitatively characterize this thermal-mending behavior. Prenotched specimens were loaded to failure under three-point bending mode; however, the specimens did not completely break into two separate pieces because of the toughening effect of PCL. Instead, the failed specimens remained connected by a ligament capable of reclosing the crack upon unloading. Specimens were then treated by being placed in a convective oven, preheated to 190 °C, for 8 min with or without a moderate external axial compression applied to promote rebonding. A second flexural test was then performed to evaluate the effect of thermal mending. In both experiments, the flexural load versus displacement curves were recorded and compared. A group of typical load−displacement curves of both the virgin and healed specimens are shown in Figure 4a−c, showing the effect of the mending pressure.

Neither the virgin nor the healed **epoxy/PCL(15.5)** specimens exhibited brittle failure; rather, cracks propagated in a comparatively slow, controlled, and reproducible fashion, and the corresponding load−displacement curves showed some degree of nonlinearity, indicating a certain degree of ductile behavior. Because the fracture toughness criteria for healing efficiency established in previous "self-healing" approaches is not valid here due to the nonbrittle behavior (2), we characterized the thermal-mending efficiency using two measures from the load−displacement curves, described in the Experimental Section: the peak area (energy) ratio and the peak force ratio. By either measure, heating alone without any compression (Figure 4a) was found to restore a large fraction of the mechanical integrity. In contrast, retesting of unhealed, fractured specimens indicated (as expected) very little strength, as shown by the short dashed curve in Figure 4a. The strain energy to failure of the thermally mended specimen exceeded that of the virgin specimen in all cases, while application of a small compressive stress parallel to the crack surface normal increased the thermal-mending efficiency significantly. In fact, mending with a compressive stress of 18.7 kPa (Figure 4c) led to strain-energy-to-failure and peak loads *exceeding* those of the virgin specimen. The thermal-mending efficiency was found to increase linearly with applied compressive stress (Figure 4d), at least for the range of stresses explored.

The surprisingly good thermal-mending performance exhibited by **epoxy/PCL(15.5)** motivated us to carry out a series of studies to reveal the underlying mechanism in detail. From our control experiment, fractured epoxy undergoing the same thermal treatment at 190 °C or even higher temperatures of 200−240 °C does not show any ability to thermally mend. Therefore, we deduce that the thermal-mending capability of **epoxy/PCL(15.5)** is not due to any residual cure of epoxy and must be the result of PCL inclusion. This is also consistent with the DSC results (Sup-

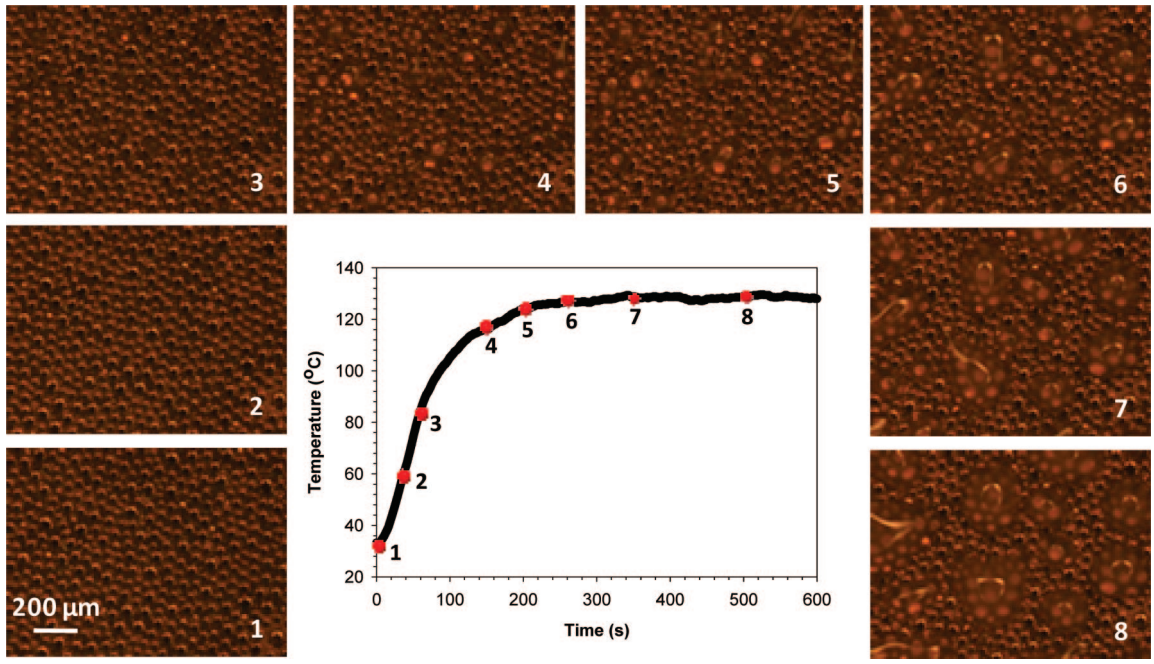

FIGURE 5. Heating-induced "bleeding" behavior. The process was characterized by hot-stage stereomicroscopy coupled with surface temperature monitoring. Sample bars were coated with a thin layer of gold (1−3 nm) to enhance the optical contrast. Images were taken at various time points (labeled on the temperature−time curve) during heating.

porting Information), which show that all epoxy/PCL samples were fully cured. On the basis of further observations and analysis, we will conclude that the thermal-mending performance is closely related to a "bleeding" phenomenon, as described below. Heating specimens to a temperature within the range $T_m^{PCL} < T < T_g^{epoxy}$ resulted in spontaneous surface wetting of samples by molten PCL—"bleeding"—as witnessed using hot-stage microscopy. Fully cured specimen bars were sputter-coated with a thin layer of gold (1−3 nm thick; to enhance optical contrast) and placed on a heated stage while under video light microscopy observation, and the surface temperature was monitored using a thermocouple. The wetting processes observed are shown as a time series in Figure 5. We observed that the bleeding is initiated with an increase in the temperature as the formation of small liquid droplets on the surface, following which the droplets grow and coalesce by contact line motion and impingement of adjacent growing droplets. Eventually (>20 min), a near-contiguous thin layer of fluid PCL covers a large area on the surface (Supporting Information). We interpret the bleeding phenomenon to be a consequence of differential thermal expansion between the two interpenetrating phases, with the minor (but continuous) PCL phase expanding at least 10% more (33) than the epoxy phase because of the melting transition itself and the large expansivity of the fluid phase (Supporting Information), schematically shown in Figure 6. We term this phenomenon "differential expansive bleeding (DEB)". We further observed that the kinetics of PCL flow to the surface expansion is mainly determined by heat transfer, with visible flow occurring in synch with the temperature rise (Figure 5 and Supporting Information). Once the temperature stabilizes, bleeding completes in a very short period of time, consistent with a calculation based on finite PCL compressibility and consequential flow through porous

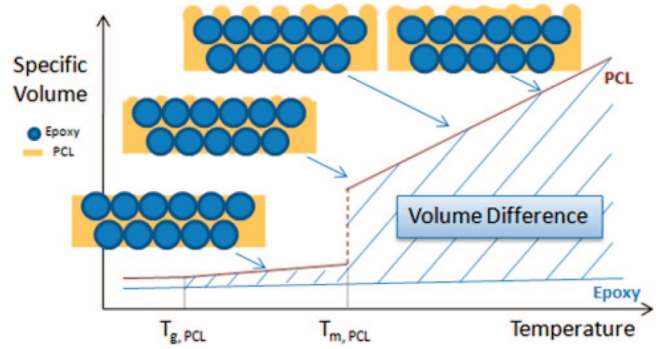

FIGURE 6. Schematic illustration of DEB indicating its origin in differential thermal expansion between PCL and epoxy.

media. PCL displays a small compressibility (large bulk modulus ~ 1 GPa), a large volume step at T_m, and a large liquid expansivity; together these result in a large transient pressure that drives the flow of liquid PCL through the network of epoxy spheres onto the surface in under 1 min. Therefore, the flow time of PCL is small compared to the time required for heat transfer. Put simply, the PCL fluid can be considered as nearly incompressible, with bleeding occurring in synch with differential thermal expansion.

To further prove the hypothesis that the observed thermal-mending performance was due to the same DEB observed at a free surface, a series of experiments were carried out to directly image the microstructural changes at the site of the SENB crack. Parts a and b of Figure 7 show the SEM images taken after the first fracture on the specimen surface and the crack surface, respectively. We observe that the specimen fractured in a "hybrid" mode: the crack propagated in a way that (1) plastically deformed matrix PCL into fibrils and finally broke them apart (ductile fracture) and (2) fractured interconnected epoxy spheres (Figure 1c), mainly through a brittle mode at the connecting planes (Figure 7b,

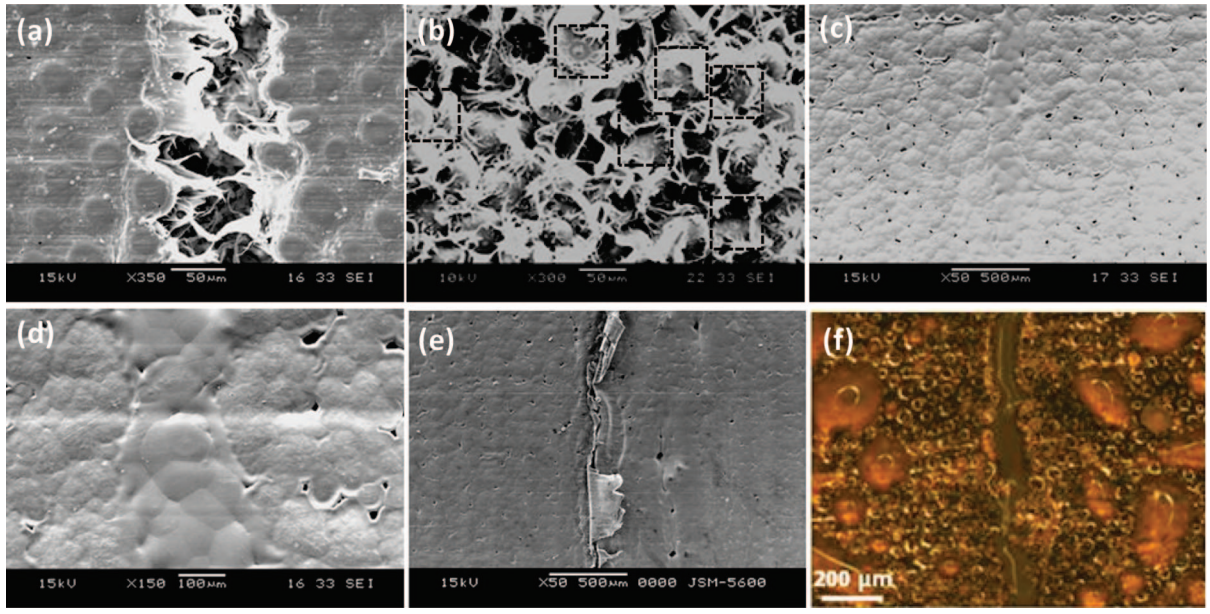

FIGURE 7. Visualization of the fracture-healing process. SEM images of (a) the crack on a completely fractured sample, (b) the fracture surface, (c and d) the cracked surface after thermal mending, and (e) the reopened crack after the fracturing of a thermally mended sample. (f) Stereooptical micrograph taken during the thermal-mending process showing the crack effectively bridged by a layer of liquid PCL melt.

dotted areas), with the bulk of the spheres remaining relatively intact. This unique fracture mode of **epoxy/PCL(15.5)** leads to a much larger apparent fracture toughness than neat epoxy. For a brief comparison, DGEBA/DDS-based epoxy with an epoxide equivalent weight similar to that used in our study has a mode I fracture toughness value of 0.7 MPa · $m^{1/2}$ (34), which corresponds to a peak load of approximately 50 N for our experimental geometry. This is much smaller than the peak loads of virgin **epoxy/PCL(15.5)** specimens (Figure 4), which are all above 200 N or 4 times larger than the neat epoxy. The appearance of the cracked region changed dramatically after thermal mending at 190 °C for 8 min. The original crack gap is no longer visible under SEM; instead, a continuous "scar" has formed in situ at the crack (Figure 7c), with the appearance of the scar resembling the structure of spherulitic crystals (Figure 7d). We reason that this scar formed by PCL bleeding to the crack surfaces, bridging the crack and subsequently crystallizing during cooling.

When the thermally mended specimen was loaded again, the crack propagated by deforming and fracturing the scar. In contrast to the first fracture, no PCL fibrils formed during the second fracture. Instead, the deformed scar was much more continuous and showed an appearance similar to that of a stretched film (Figure 7e), and some portions buckled because of the crack closure at the end of test, induced by the remaining elastic response of the ligament. The stereooptical micrograph taken during the thermal-mending process clearly shows the presence of a liquid PCL layer bridging the crack (Figure 7f). These observations are also consistent with our fracture experiments (Figure 4a–c), in which all thermally mended samples display a long "tail" (postpeak load decay) in load–displacement curves, with much higher ultimate displacements than the virgin samples. This indicates a change toward a more ductile failure, while we associate with the tough, semicrystalline PCL "scar" that formed in the crack during mending. For clarity purposes, Figure 8 schematically illustrates the overall mechanism of thermal mending based on all of the observations and analysis. The thermally induced "bleeding" produces a PCL layer bridging the crack, which subsequently recrystallizes to form a tough "scar" restoring the mechanical strength to a significant extent.

Finally, we have utilized the DEB phenomenon of **epoxy/PCL(15.5)** for function as a rigid adhesive with excellent reversibility of adhesion. This is demonstrated in Figure 9a. A specimen bar was first heated on a hot plate for several minutes, gently put on top of another specimen, and subsequently allowed to cool down to room temperature. A very strong bonding that was able to withstand a 200 g standard weight (about 100 times the specimen mass) was formed between the two surfaces by recrystallization of the DEB-extruded PCL layer, a mechanism similar to that of "scar" formation discussed before. A distinguishing difference of our material compared to conventional hot-melt adhesives is that a high modulus was maintained at the "adhesive" state (rigid adhesive) and there was no requirement for significant thinning of the bonding material. Furthermore, we observed that the bonded blocks could be easily debonded by heating ($T > T_m$) to melt the PCL crystals, as shown in Figure 9a.

To quantify this adhesion, butt-joint experiments were conducted where two sample bars bonded at their ends and loaded to failure under tensile mode (as the inset of Figure 9b indicates) while collecting the load versus displacement data. Figure 9b shows the results for two bonded specimens both prepared by heating at 150 °C for 9 min using a spring-based bonding device (detailed procedure for bonding described in the Experimental Section; a photograph of the bonding device is available in the Supporting Information).

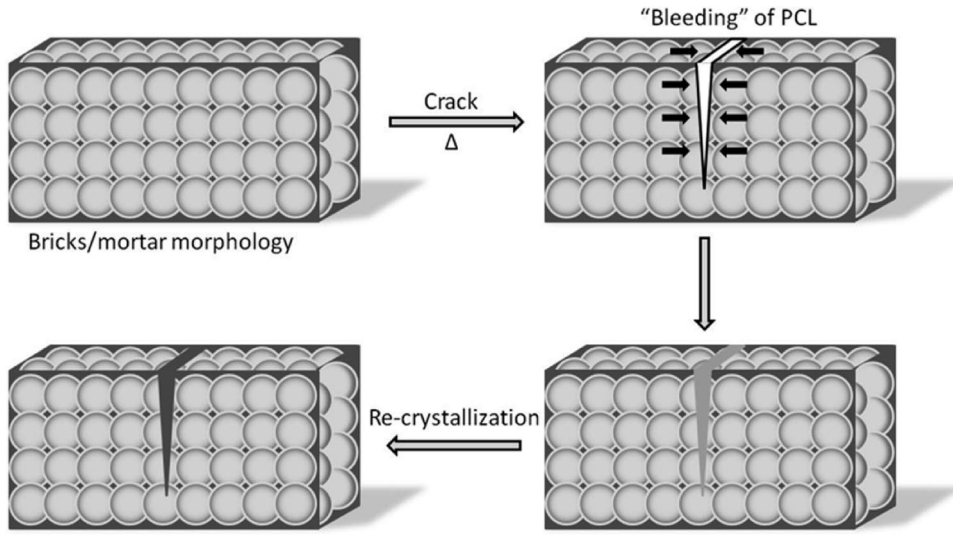

FIGURE 8. Schematic illustration of the overall mechanism of thermal mending.

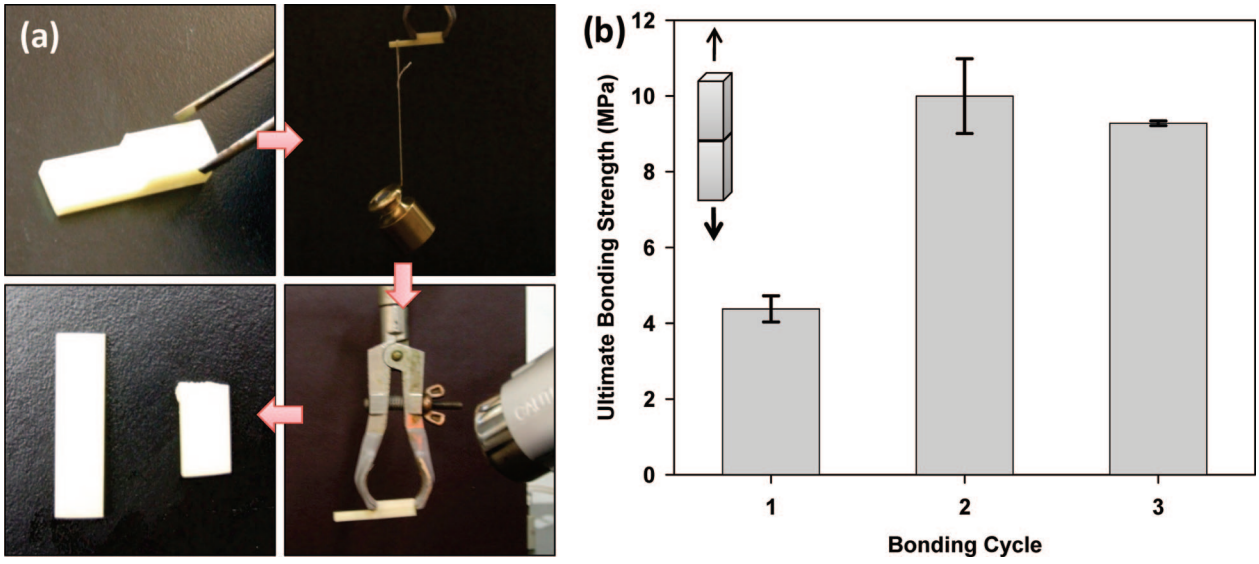

FIGURE 9. Demonstration of the application as a rigid adhesive with reversible adhesion. (a) Sample bar first heated on a hot plate for several minutes, gently put on top of another sample, and allowed to cool. A strong bonding was formed between the two sample surfaces and can withstand flexure from hanging of a standard weight of 200 g. The adhesion was removed upon heating with a heat gun for less than 1 min, and the two samples detached instantaneously. (b) Butt-joint experimental results for two samples bonded at 150 °C for 9 min up to three bonding cycles.

Here the ultimate bonding strength is defined as the highest load achieved normalized by the sample cross-sectional area (5 mm × 10 mm). Neat epoxy did not yield any detectable self-adhesion, while surprisingly high bonding strengths (>8 MPa) were achieved with **epoxy/PCL(15.5)** and no significant decay was observed through three bonding cycles. Indeed, the second bonding produced a much stronger adhesion than the first bonding, a finding we attribute to PCL enrichment at the surface during the first fracture and in the form of fibrils pulled from within the bricks/mortar microstructure. Because both thermal-mending and reversible adhesion are of a similar DEB origin, we expect that thermal mending can also be conducted repeatedly, although this is a subject to be studied in the future. In addition to bonding to the same material, a heated **epoxy/PCL(15.5)** sample was found to bond equally strong to various substrates, including aluminum, steel, and conventional glass, and a detailed study on such adhesion is underway.

CONCLUSIONS

To conclude, we have demonstrated that a "bricks and mortar" epoxy/PCL blend features unique differential expansive "bleeding" that enables excellent thermal-mending performance and applicability as a rigid and reversible adhesive. Similar morphologies are achievable in a large number of other systems, where a thermoset is blended with an amorphous (35–38) or semicrystalline (39, 40) thermoplastic polymer; therefore, we envision broad applicability of this strategy to the design of DEB polymers and polymer composites, based on low raw materials cost and ease of manufacturing, for those applications requiring long-lasting materials performance and facile repair. Further, the reversible adhesive properties of DEB polymer composites should

enable a new paradigm in adhesives as reusable bonding "blocks" that can adhere to or be removed from virtually any surface with a simple heat treatment.

Acknowledgment. The authors gratefully acknowledge Dr. Kun Li (Syracuse University) and Dr. Jeff Baur and Dr. Ed Foster (Air Force Research Laboratory, Wright Patterson AFB, OH) for insightful discussions. Financial support was provided by a Small Business Innovation Research (SBIR) program contract to NEI Corp. from the U.S. Air Force Research Laboratory (Contract No. FA8651-07-C-0105). The authors thank technical contract monitor Dr. Michael Valentino for his insights. Finally, the authors thank Prof. Richard Lehman (Rutgers University) and Dr. Kenneth Mann (SUNY Upstate Medical University) for use of their mechanical testing equipment during this study.

Supporting Information Available: DSC thermograms of epoxy/PCL blends of various compositions (Figure S1), DMA results for three epoxy/PCL blends (**epoxy/PCL(4.3)**, **epoxy/PCL(11.5)**, and **epoxy/PCL(34.9)**) (Figure S2), comparison of dimensional stabilities of **epoxy/PCL(15.5)** and pure PCL (Figure S3), a stereooptical micrograph showing a heated surface of **epoxy/PCL(15.5)** after DEB reached steady state (>20 min) (Figure S4), a photograph showing the bonding device used for preparing butt-joint specimens (Figure S5), and calculation of the flow time, t_{flow}, for DEB (Figure S6). This material is available free of charge via the Internet at http://pubs.acs.org.

REFERENCES AND NOTES

(1) Kessler, M. R.; Sottos, N. R.; White, S. R. *Composites, Part A* **2003**, *34*, 743–753.
(2) Rule, J. D.; Brown, E. N.; Sottos, N. R.; White, S. R.; Moore, J. S. *Adv. Mater.* **2005**, *17*, 205–208.
(3) White, S. R.; Sottos, N. R.; Geubelle, P. H.; Moore, J. S.; Kessler, M. R.; Sriram, S. R.; Brown, E. N.; Viswanathan, S. *Nature* **2001**, *409*, 794–797.
(4) Wilson, G. O.; Moore, J. S.; White, S. R.; Sottos, N. R.; Andersson, H. M. *Adv. Funct. Mater.* **2008**, *18*, 44–52.
(5) Keller, M. W.; White, S. R.; Sottos, N. R. *Adv. Funct. Mater.* **2007**, *17*, 2399–2404.
(6) Cho, S. H.; Andersson, H. M.; White, S. R.; Sottos, N. R.; Braun, P. V. *Adv. Mater.* **2006**, *18*, 997–1000.
(7) Pang, J. W. C.; Bond, I. P. *Compos. Sci. Technol.* **2005**, *65*, 1791–1799.
(8) Williams, G.; Trask, R.; Bond, I. *Composites, Part A* **2007**, *38*, 1525–1532.
(9) Williams, H. R.; Trask, R. S.; Bond, I. P. *Smart Mater. Struct.* **2007**, *16*, 1198–1207.
(10) Yin, T.; Rong, M. Z.; Zhang, M. Q.; Yang, G. C. *Compos. Sci. Technol.* **2007**, *67*, 201–212.
(11) Yuan, Y. C.; Rong, M. Z.; Zhang, M. Q.; Chen, J.; Yang, G. C.; Li, X. M. *Macromolecules* **2008**, *41*, 5197–5202.
(12) Toohey, K. S.; Sottos, N. R.; Lewis, J. A.; Moore, J. S.; White, S. R. *Nat. Mater.* **2007**, *6*, 581–585.
(13) Chen, X. X.; Dam, M. A.; Ono, K.; Mal, A.; Shen, H. B.; Nutt, S. R.; Sheran, K.; Wudl, F. *Science* **2002**, *295*, 1698–1702.
(14) Cordier, P.; Tournilhac, F.; Soulie-Ziakovic, C.; Leibler, L. *Nature* **2008**, *451*, 977–980.
(15) Caruso, M. M.; Delafuente, D. A.; Ho, V.; Sottos, N. R.; Moore, J. S.; White, S. R. *Macromolecules* **2007**, *40*, 8830–8832.
(16) Hayes, S. A.; Jones, F. R.; Marshiya, K.; Zhang, W. *Composites, Part A* **2007**, *38*, 1116–1120.
(17) Gupta, S.; Zhang, Q. L.; Emrick, T.; Balazs, A. C.; Russell, T. P. *Nat. Mater.* **2006**, *5*, 229–233.
(18) Kessler, M. R. *Proc. Inst. Mech. Eng., Part G* **2007**, *221*, 479–495.
(19) Bergman, S. D.; Wudl, F. *J. Mater. Chem.* **2008**, *18*, 41–62.
(20) Wool, R. P. *Soft Matter* **2008**, *4*, 400–418.
(21) Wu, D. Y.; Meure, S.; Solomon, D. *Prog. Polym. Sci.* **2008**, *33*, 479–522.
(22) Yuan, Y. C.; Yin, T.; Rong, M. Z.; Zhang, M. Q. *eXPRESS Polym. Lett.* **2008**, *2*, 238–250.
(23) Kim, J. Y.; Cho, C. H.; Palffy-Muhoray, P.; Mustafa, M.; Kyu, T. *Phys. Rev. Lett.* **1993**, *71*, 2232–2235.
(24) Kiefer, J.; Hilborn, J. G.; Hedrick, J. L. *Polymer* **1996**, *37*, 5715–5725.
(25) Kim, J. W.; Lee, K. S.; Ju, H. K.; Ryu, J. H.; Han, S. H.; Chang, I. S.; Kang, H. H.; Oh, S. G.; Suh, K. D. *J. Polym. Sci., Part A: Polym. Chem.* **2004**, *42*, 2202–2213.
(26) Girard-Reydet, E.; Sautereau, H.; Pascault, J. P.; Keates, P.; Navard, P.; Thollet, G.; Vigier, G. *Polymer* **1998**, *39*, 2269–2279.
(27) Inoue, T. *Prog. Polym. Sci.* **1995**, *20*, 119–153.
(28) Williams, R. J. J.; Rozenberg, B. A.; Pascault, J. P. *Adv. Polym. Sci.* **1997**, *128*, 95–156.
(29) Chen, J. L.; Chang, F. C. *Macromolecules* **1999**, *32*, 5348–5356.
(30) Ni, Y.; Zheng, S. X. *Polymer* **2005**, *46*, 5828–5839.
(31) Vanden Poel, G.; Goossens, S.; Goderis, B.; Groeninckx, G. *Polymer* **2005**, *46*, 10758–10771.
(32) Barone, L.; Carciotto, S.; Cicala, G.; Recca, A. *Polym. Eng. Sci.* **2006**, *46*, 1576–1582.
(33) Rodgers, P. A. *J. Appl. Polym. Sci.* **1993**, *48*, 1061–1080.
(34) Kishi, H.; Shi, Y. B.; Huang, J.; Yee, A. F. *J. Mater. Sci.* **1997**, *32*, 761–771.
(35) Cabanelas, J. C.; Serrano, B.; Baselga, J. *Macromolecules* **2005**, *38*, 961–970.
(36) Meynie, L.; Fenouillot, F.; Pascault, J.-P. *Polymer* **2004**, *45*, 1867–1877.
(37) Oyanguren, P. A.; Galante, M. J.; Andromaque, K.; Frontini, P. M.; Williams, R. J. J. *Polymer* **1999**, *40*, 5249–5255.
(38) Wang, M.; Yu, Y.; Wu, X.; Li, S. *Polymer* **2004**, *45*, 1253–1259.
(39) Goossens, S.; Groeninckx, G. *Macromolecules* **2006**, *39*, 8049–8059.
(40) Johnsen, B. B.; Kinloch, A. J.; Taylor, A. C. *Polymer* **2005**, *46*, 7352–7369.

AM8001605